Currents driven by a steady uniform wind stress on the shelf seas around the British Isles

Wind currents
Model
North Sea
Celtic Sea
English Channel

Courants dus au vent
Modèle
Mer du Nord
Mer Celtique
Manche

R. D. Pingree [a], D. K. Griffiths [b].
[a] Institute of Oceanographic Sciences, Wormley, Surrey, UK.
[b] The Laboratory Marine Biological Association, Citadel Hill, Plymouth, UK.

Received 26/9/79, in revised form 7/1/80, accepted 11/1/80.

ABSTRACT

A numerical model is used to derive the currents driven by a steady wind stress on the shelf seas around the British Isles. Water budgets for the North Sea and Celtic Sea are derived for varying wind directions and the dynamical significance of the derived circulations is discussed.

Oceanol. Acta, 1980, **3**, 2, 227-236.

RÉSUMÉ

Courants engendrés par un vent permanent sur le plateau continental entourant la Grande-Bretagne

Un modèle numérique est utilisé pour déterminer les courants engendrés par un vent permanent sur le plateau continental autour de la Grande-Bretagne. Les bilans de masse d'eau pour la Mer du Nord et la Mer Celtique sont déduits pour des directions du vent variables et la signification dynamique des circulations trouvées est discutée.

Oceanol. Acta, 1980, **3**, 2, 227-236.

INTRODUCTION

A numerical model is used to derive the currents driven by a steady wind stress on the shelf seas around the British Isles (Fig. 1). The numerical grid for the area also includes the Skagerrak and Kattegat as these regions have a marked influence on the flow in the North Sea. The currents derived from the numerical model are the average values for the water column and will be most relevant during the winter when conditions are mostly well mixed.

The vertically integrated equations of motion and continuity are conveniently expressed in vector form:

- continuity

$$\frac{\partial E}{\partial t} + \nabla . D\mathbf{u} = 0, \qquad (1)$$

- momentum

$$\frac{\partial \mathbf{u}}{\partial t} + \mathbf{u}.\nabla \mathbf{u} + 2\boldsymbol{\Omega} \wedge \mathbf{u} = -g\nabla E - \frac{1}{\rho}\nabla P_a - \frac{\tau_B}{\rho D} + \frac{\tau_w}{\rho D} + K_H \nabla^2 \mathbf{u}, \qquad (2)$$

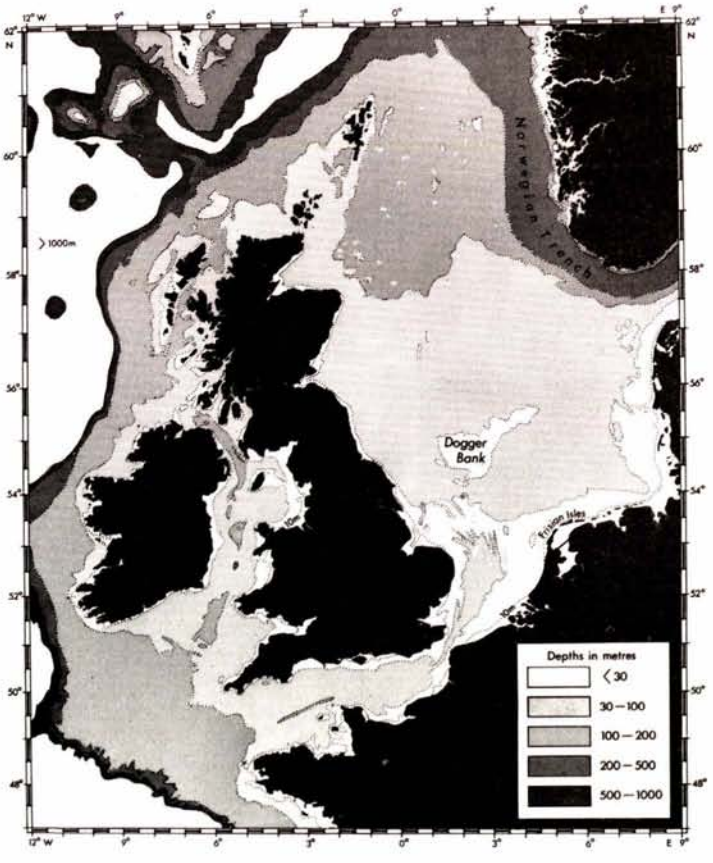

Figure 1
Bottom topography of the North west European Shelf.

where

$$D=h+E. \quad (3)$$

$$\tau_B=\rho C_D|\mathbf{u}|\mathbf{u}, \quad (4)$$

(see Table 1 for the definition of the symbols used).

Horizontal diffusion ($K_H \sim 10^6\ cm^2.s^{-1}$) even for the smallest wave numbers and numerical averaging for the grid scale of this model are generally small compared with the other terms in the momentum equation and are excluded from the following discussion.

These equations were transformed into spherical polar coordinates and used in finite difference form taking account of variations of the Coriolis parameter with latitude (see Flather and Davies, 1975) to determine both the tidal (Weare, 1975) and the wind driven currents (Ronday, 1972; Maier-Reimer, 1977) on the shelf sea around the British Isles.

THE NUMERICAL MODEL

Boundary conditions

Meteorological

A steady wind stress was imposed on a working model of the M_2 tide on the north west European continental shelf. The wind stress, τ_w, can be assumed to be related to the wind, $\mathbf{w}_{10}$, at a height of 10 m, by the relation

$$\tau_w=\rho_a C_{10}\mathbf{w}_{10}|\mathbf{w}_{10}|. \quad (5)$$

A wind speed of 10 ms^{-1} with a value of $C_{10} \sim 1.3\times10^{-3}$ (see Phillips, 1966) gives a wind stress of

$$\tau_w=1.6\ dynes.cm^{-2},$$

and this value was used in equation (2) for most of the computed values. The results are derived in terms of wind stress rather than wind velocity so that they are independent of the exact form of the relationship between the drag coefficient and the wind speed. Bowden (1956) inferred that the mean coefficient of wind stress might be as large as 4.5×10^{-3} from his study of the flow of water through the Strait of Dover.

If the wind is assumed to be in an approximate geostrophic balance with the atmospheric pressure, then the pressure field, P_a, is also defined by the wind velocity through the geostrophic relation

$$2\boldsymbol{\Omega}\wedge\mathbf{w}_{10}=-\frac{1}{\rho_a}\nabla P_a. \quad (6)$$

The relative dynamical importance of atmospheric pressure with respect to wind stress, which is proportional to the square of wind speed [see (5)], thus decreases with increasing wind speed (Hunter, 1974).

In large scale frictionless systems the atmospheric pressure gradient may drive a geostrophically balanced current. In smaller scale partially enclosed seas the sea surface slope can adjust to balance the atmospheric pressure gradient before a geostrophically balanced flow can develop. In the absence of wind stress, the steady state form of (2) then becomes

$$0=-g\nabla E_a-\frac{1}{\rho}\nabla P_a, \quad (7)$$

which also defines the open sea boundary conditions for the sea surface elevation, E_a, due to atmospheric pressure. The appropriateness of this inverted barometer boundary condition was tested by running the numerical model with the pressure gradient term in equation (2) defined by (6) above for a west wind of 10 ms^{-1}. It was confirmed that the residual currents generated solely from an applied pressure field in the absence of wind stress fall away to zero after a few tidal cycles provided condition (7) is applied at the open sea boundaries for the sea surface elevations.

It is convenient therefore to subtract equation (7) from equation (2) thereby eliminating the atmospheric pressure term to give

$$\frac{\partial\mathbf{u}}{\partial t}+\mathbf{u}.\nabla\mathbf{u}+2\boldsymbol{\Omega}\wedge\mathbf{u}=-g\nabla E-\frac{\tau_B}{\rho D}+\frac{\tau_w}{\rho D}. \quad (8)$$

The open sea boundary condition at the shelf break now becomes $\bar{E}=0$, and elsewhere $\bar{E}$ refers to the steady state adjustment of the sea surface in the absence of effects due to atmospheric pressure. If coastal flooding is of interest then it is important to add the atmospheric contribution to the mean sea level [see equation (7)]. If upwelling is of interest then the derived sea level distributions will be more relevant, though of course a depth integrated model will provide no information on the vertical circulations that may develop.

Tidal

The tidal flow was driven by M_2 tidal elevations specified at the edge of the continental shelf and these were obtained from records of moored gauges (Cartwright, 1976; Flather, 1976). The derived M_2 tidal elevations were accurate to about 5° in phase and 10 cm in amplitude (standard deviation) using an optimum fixed drag coefficient of $C_D=0.0025$. The M_2 tidal flow determines the friction for the wind driven currents where the M_2 tidal currents are larger than the wind driven residual flows. However there are some important regions (for example SW Ireland and Skagerrak) where the wind driven currents are much larger than the oscillating tidal flow and the advantages of first averaging the tidal solution noted by some authors is offset by the fact that in these areas the friction is determined by the wind driven currents.

At the coastline the normal velocity was set equal to zero. The numerical grid was 5′ of latitude and 10′ of longitude giving some 26×10^3 points of which about half were sea areas where currents and elevations were determined (Pingree, Griffiths, 1978). The model ran without numerical instability with a time step of 1 minute.

Convergence

Three time scales are involved in determining the steady state wind residuals. First, for convenience, the averaging period must be a complete tidal cycle, T, so as to remove any oscillating tidal contribution from the residuals.

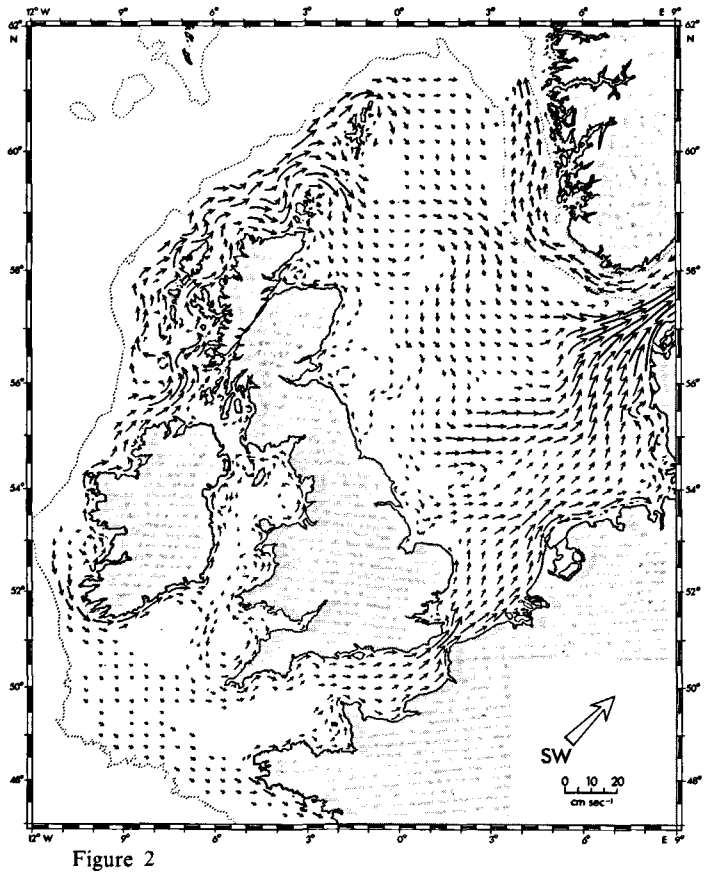

Figure 2

The wind driven residual currents resulting from a uniform SW wind stress of 1.6 *dynes* cm^{-2}. *The length of a current vector determines the strength of the current at its central point. The current arrows are slightly curved to conform with the direction of current flow. Only about one tenth of the current vectors have been drawn and values less than* 1.25 $cm.s^{-1}$ *have been omitted.*

Figure 3

The sea level corresponding to the SW wind residuals shown in Figure 2 *(cm).*

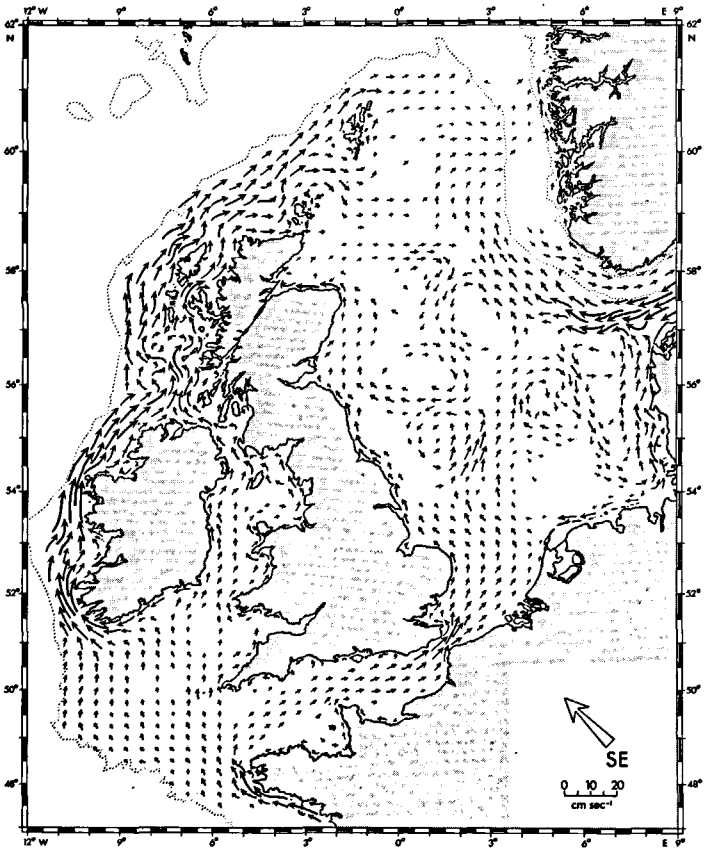

Figure 4

The wind driven residual currents resulting from a uniform SE wind stress of 1.6 *dynes* cm^{-2}. *(Arrows drawn as for Figure* 2*).*

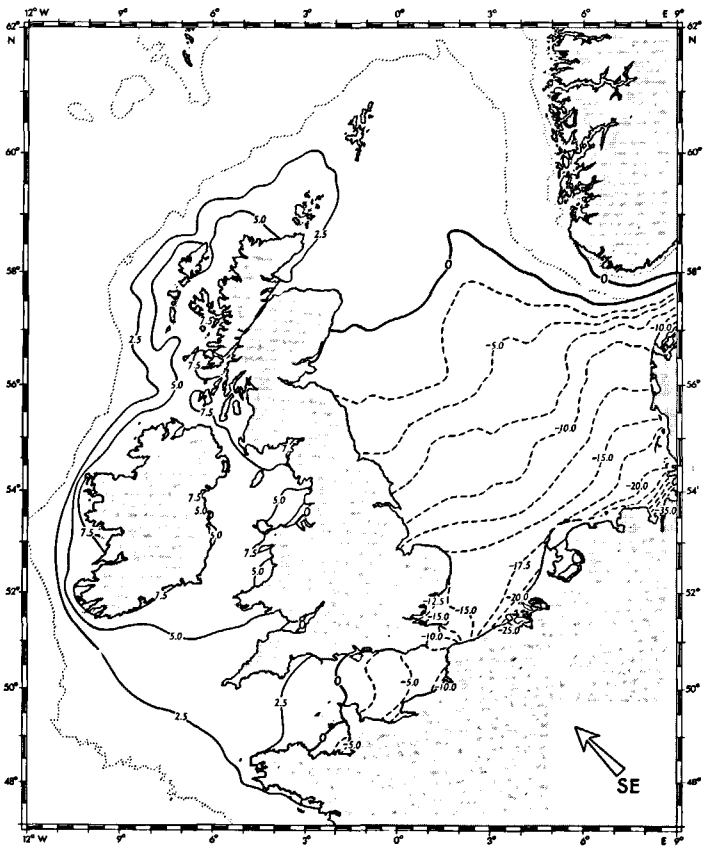

Figure 5

The sea level corresponding to the SE wind residuals shown in Figure 4 *(cm).*

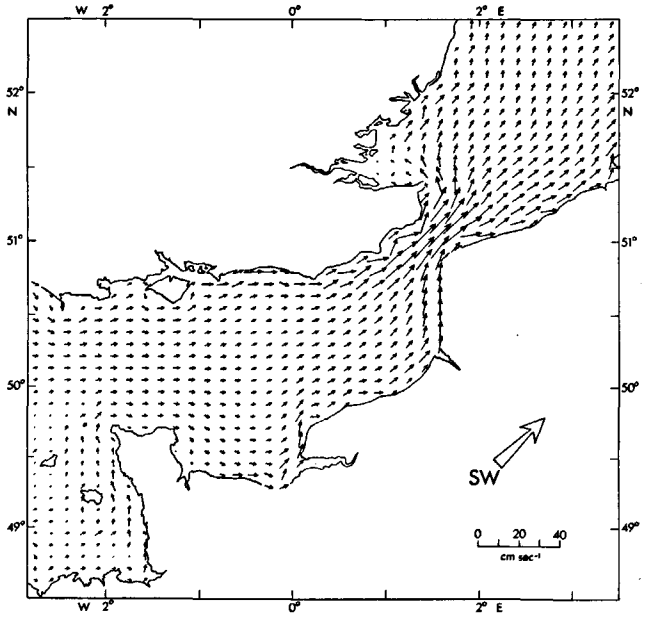

Figure 6

Increased resolution under SW wind conditions (see Fig. 2) showing flow through the Dover Strait from the English Channel into the Southern Bight of the North Sea. The arrows are centred as in Figure 2 but not curved.

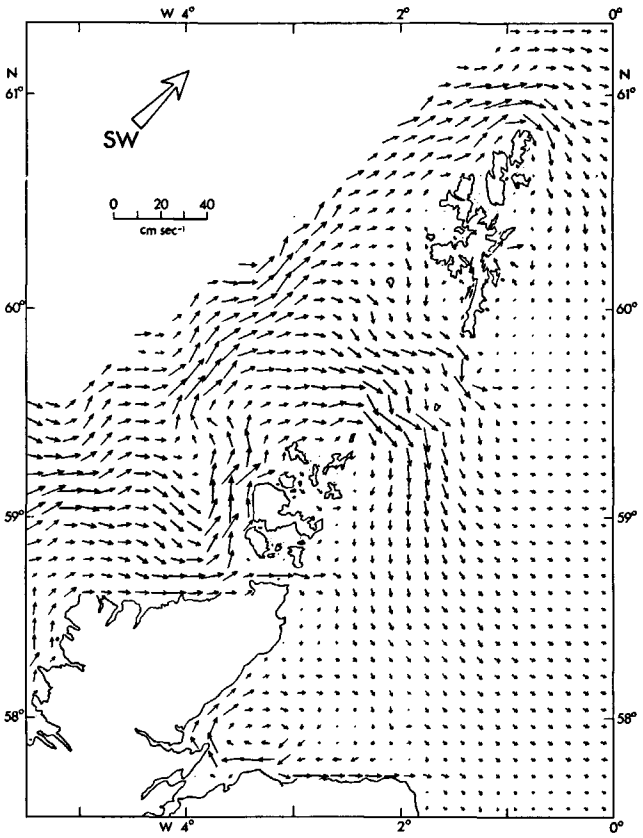

Figure 7

Increased resolution under SW wind conditions (see Fig. 2) showing flow through the Fair Isle Channel into the Northern North Sea.

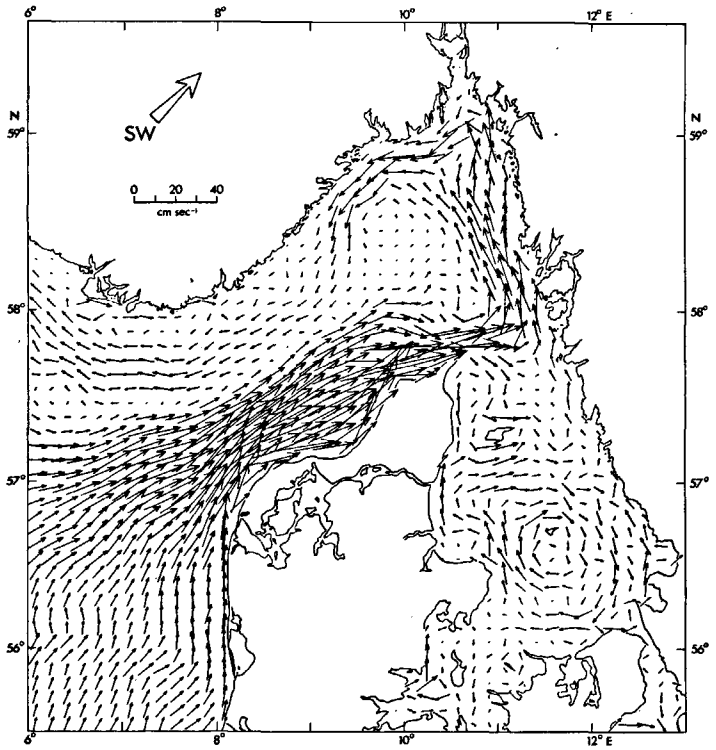

Figure 8

Increased resolution under SW wind conditions (see Fig. 2) showing flow in the Skagerrak and Kattegat. Most of the flow entering the North Sea through the Dover Strait and the Fair Isle Channel passes around the Skagerrak and out along the Norwegian Trench.

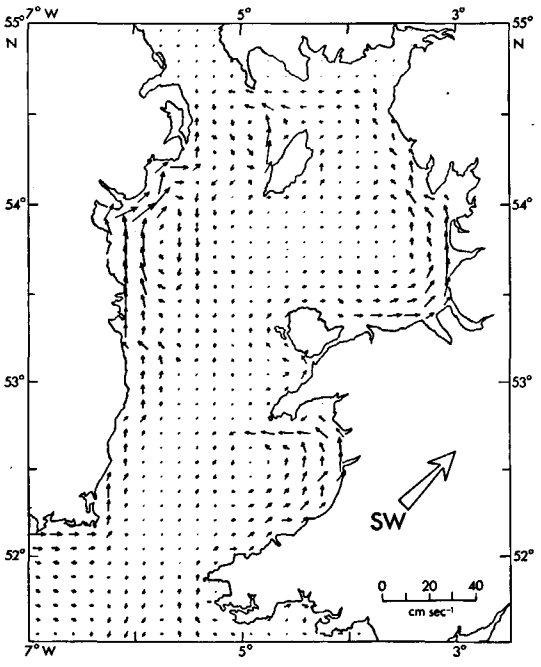

Figure 9

Increased resolution under SW wind conditions (see Fig. 2) showing minimal flow through the St. Georges Channel and the wind driven circulations in the Irish Sea.

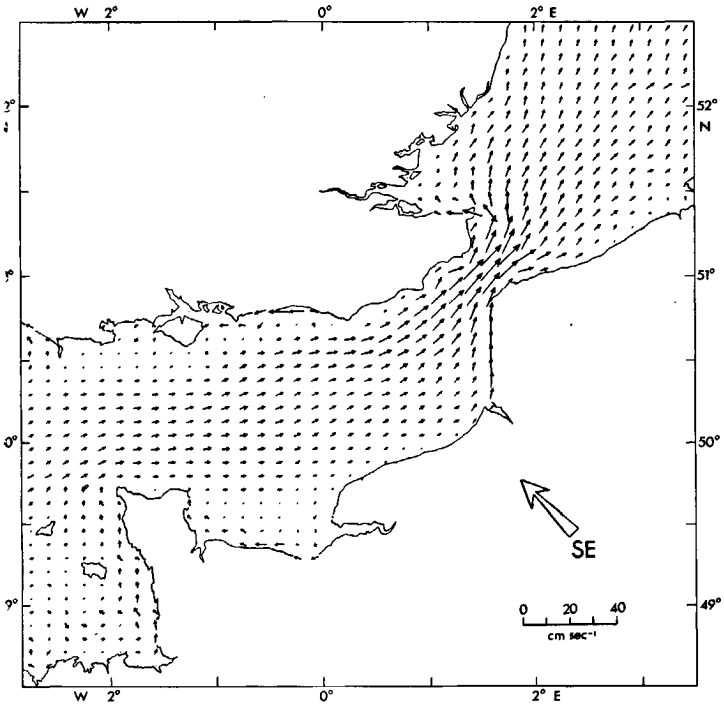

Figure 10

Increased resolution under SE wind conditions (see Fig. 4) showing flow through the Dover Strait from the English Channel into the Southern Bight of the North Sea. The arrows are centred as in Figure 4, but not curved.

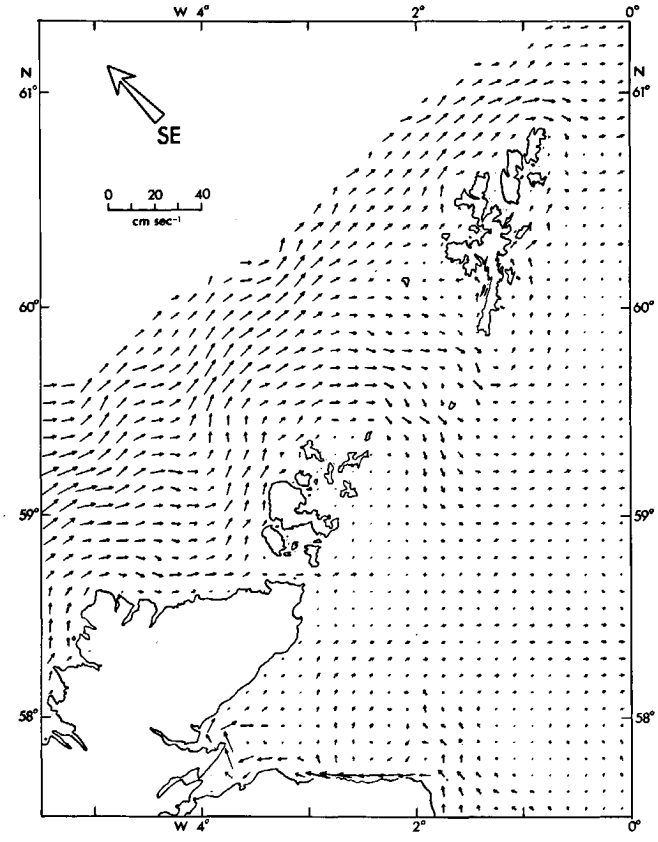

Figure 11

Increased resolution under SE wind conditions (see Fig. 4) showing flow through the Fair Isle Channel into the Northern North Sea.

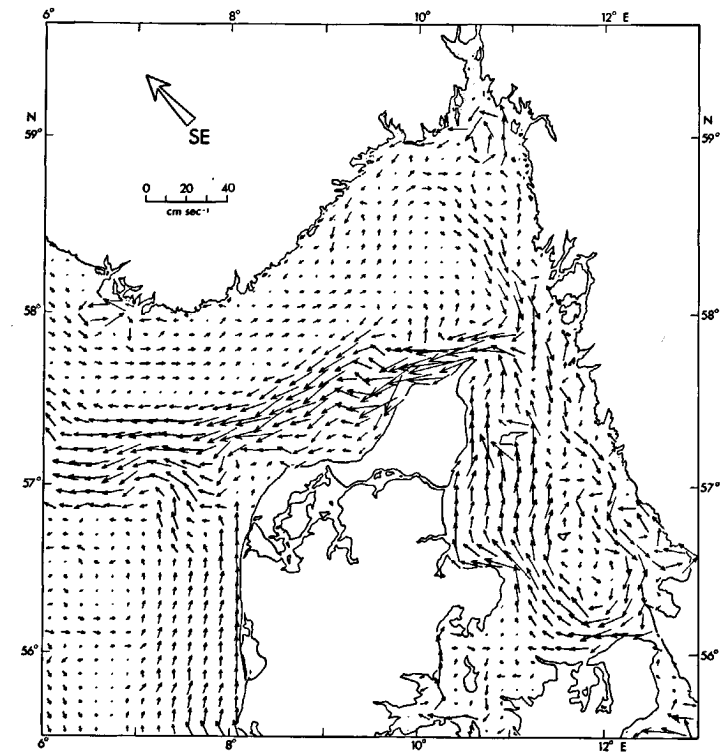

Figure 12

Increased resolution under SE wind conditions (see Fig. 4) showing flow in the Skagerrak and Kattegat.

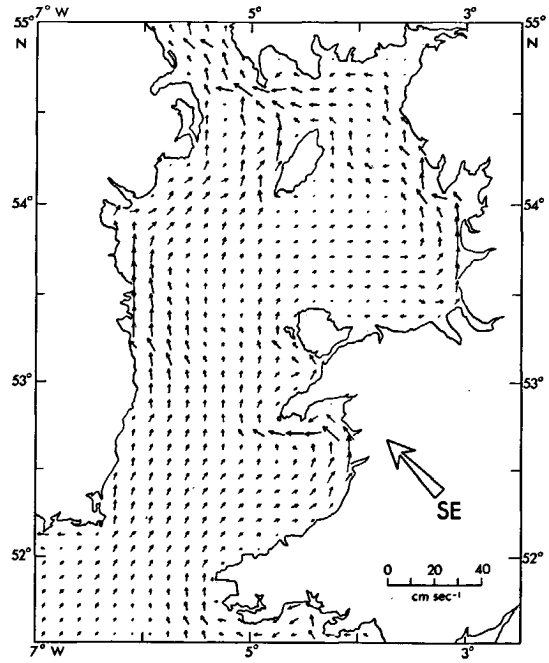

Figure 13

Increased resolution under SE wind conditions (see Fig. 4) showing flow through the St. Georges Channel and the Irish Sea.

The time scales determining convergence of the numerical solutions are the dissipation time scale, T_D, and the time, T_L, taken for long waves to travel through the geographical extent, L, of the modelled region. These may be defined approximately as follows:

$$T_D \sim \frac{h}{C_D \hat{u}_T} \sim \frac{50 \times 10^2}{2.5 \times 10^{-3} \times 50} \sim T \qquad (9)$$

and

$$T_L \sim \frac{L}{\sqrt{gh}} \sim 2T. \qquad (10)$$

These criteria guarantee rapid convergence after a few tidal cycles and are incidentally the reason why the tidal solution itself reaches reasonable convergence in a few tidal cycles. In accordance with these considerations a steady wind stress was applied for only 5 tidal cycles starting from the tidal solution without wind residuals, although satisfactory convergence was generally achieved after three tidal cycles. Inertial oscillations with period $T_p = 2\pi/f$ ($f = 2\Omega \sin \varphi$) due to the suddenly imposed wind stress also decay rapidly by virtue of (9) in shallow water.

RESULTS

A steady wind was blown for five tidal cycles after which time the sea levels and residual flows due to wind forcing were determined by averaging over a tidal cycle and then subtracting the tidal residuals. The results for a SW wind and a SE wind together with their corresponding changes in sea level are shown in Figures 2, 3, 4, 5. More detailed flow patterns in individual passages, the Dover Strait, the Fair Isle channel (between the Orkney and Shetland Isles), the Skagerrak and the St. Georges Channel are illustrated in Figures 6, 7, 8, 9 for a SW wind stress and Figures 10, 11, 12, 13 for a SE wind stress.

The main difference between these results and previous results can be illustrated by comparing estimates for the transport of water through the Strait of Dover. Prandle (1978) and Oerleman (1978) give results differing by 25% for the transport through the Strait of Dover for the same wind stress for a similar modelled region of limited geographical extent. Whereas both Prandle and Oerleman give a maximum response for a wind from a direction 203° our results suggest a maximum response for a wind from 187° and also show considerably increased flow through the Dover Strait (Fig. 14). These discrepancies occur because sea level differences set up by the effect of the wind stress on the North Sea and the Celtic Sea are difficult to take into account when estimating the transport from reduced models and so for each computed steady flow, a correction must be applied for sea level differences set up in other regions. A complete shelf model accounts for sea level differences over a much increased region. The reduced value of 187° reflects the extended direction to the open sea of the median line of the North Sea. Of course these open sea boundary conditions are not fully eliminated here but simply removed further away from the regions of key interest.

Figure 14

A comparison of the transport through the Dover Strait with other models for varying wind directions.

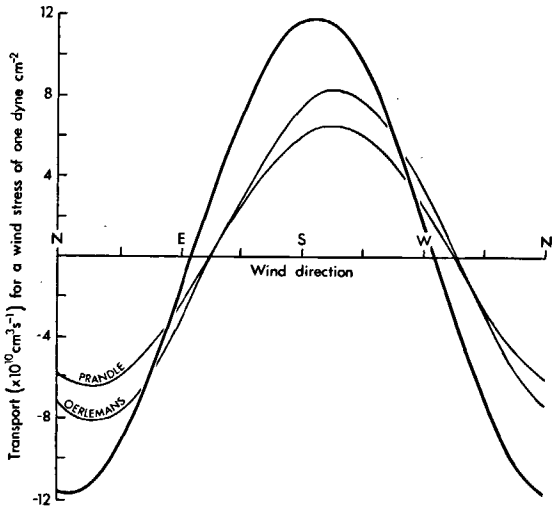

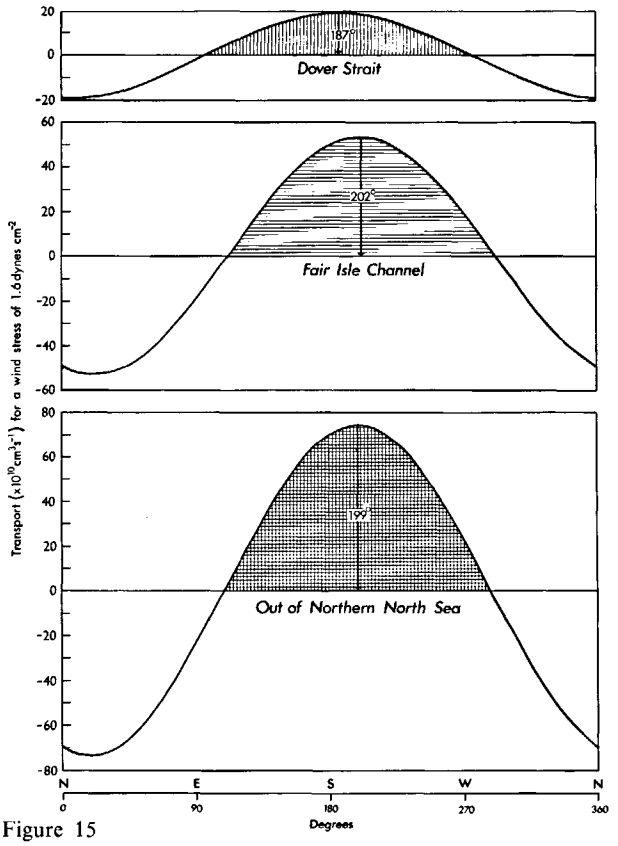

Figure 15

Transport response functions for varying wind directions making up the total wind driven water budget for the North Sea; (a) through the Strait of Dover into the North Sea; (b) through the Fair Isle Channel (and Pentland Firth) into the North Sea; (c) out of the Northern North Sea across a section from the Shetland Isles to Norway.

Similar difficulties (irrespective of the numerical scheme) have generally been experienced when estimating tidal residuals from models of limited geographical area. In addition to the wind transport there is a tidally induced residual flow through the Strait of Dover to the North Sea. Our value of 3×10^4 m^3.s^{-1} is less than half the value determined by Prandle (1978 *a*). The tidal residual was equally small through the Irish Sea (northwards) $\sim 2 \times 10^4$ m^3.s^{-1}.

A water budget for the North Sea can be made by considering the transport of water through the Dover Strait, through the Fair Isle Channel and across a section from the Shetland Isles to the Norwegian coast, Figure 15.

The transports, Q, due to both wind and tide, in units of $10^{10}\,cm^3.s^{-1}$ can be summarised in terms of the direction of the wind, Θ, and the magnitude of the wind stress, τ_w, in dynes.cm^{-2}, as follows:

$$Q = 3 + 12\,\mathrm{Cos}\,(\Theta - 187°)\,|\,\tau_w\,|\,.$$

Eastward through the English Channel into the North Sea and

$$Q = -4 + 33\,\mathrm{Cos}\,(\Theta - 202°)\,|\,\tau_w\,|$$

through the Fair Isle Channel into the North Sea to give

$$Q = 45\,\mathrm{Cos}\,(\Theta - 199°)\,|\,\tau_w\,|$$

across a section from the Shetland Isles to Norway. The transport northwards through the Irish Sea (Fig. 16) of

$$Q = 2 + 10\,\mathrm{Cos}\,(\Theta - 140°)\,|\,\tau_w\,|$$

together with the flow through the Strait of Dover gives the transport

$$Q = 6 + 20\,\mathrm{Cos}\,(\Theta - 166°)\,|\,\tau_w\,|$$

across the Celtic Sea.

These relationships are valid for steady winds from a constant direction over the whole of the modelled region. Although such conditions may rarely be met in nature it is of interest to examine the resulting distributions of currents and elevations from a physical point of view and these aspects are examined in more detail in the next section. It is of course possible to derive from the model the time varying transports with real winds over the modelled region and application of numerical models to storm surge predictions have been described by Flather and Davies (1975).

The derived steady distributions of currents and sea surface elevations will be important in establishing the residual wind driven circulations for the North West European continental shelf. The numerical results show that the wind driven currents are nearly linear with respect to the applied wind stress (see later). The actual long term residual flows will then be approximately represented by the model results using the long term residual wind stress. The residual wind stress is not accurately known but expected to be about SW and reasonably spatially uniform.

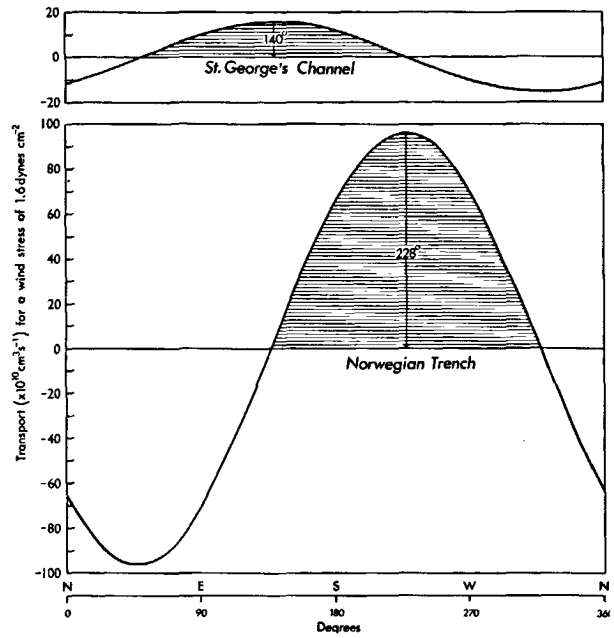

Figure 16

Transport response functions for varying wind directions; (a) through the St. Georges Channel and into the Irish Sea. (b) northwards across a section of the Norwegian Trench at 59°30′N.

DISCUSSION

Dynamic considerations

Linearity

Consider a wind driven component with frequency, σ, and wave number, k. Then as steady state conditions are approached the frequency ratio, σ/f, tends to zero and it is possible to neglect accelerations arising from the term, $d\mathbf{u}/dt$, with respect to the Coriolis acceleration provided the Rossby Number, R_0, is also small, where

$$R_0 = \frac{\mathbf{u}.\nabla\mathbf{u}}{2\boldsymbol{\Omega}\wedge\mathbf{u}} \sim k\,|\,\mathbf{u}\,|\,/f. \qquad (11)$$

For maximum values of R_0 with wave number say of order $0.1\,km^{-1}$ and residual currents, $\bar{\mathbf{u}}$, as large as $100\,cm.s^{-1}$ $R_0 \sim 1$ and so non-linear effects, due to the advection of momentum, are often small even for quite large wind stresses.

Since, in addition, the bottom friction term is either small or essentially linear then the equation describing the steady state wind residuals is also linear. Linearisation of the quadratic form of bottom friction will be a good approximation provided the tidal stream amplitude, $\hat{u}_T$, is large compared with the residual current due to the wind, $\bar{\mathbf{u}}$ (Hunter, 1975; Heaps, 1978). The mean bottom friction, $\bar{\tau}_B$, defined as

$$\bar{\tau}_B = \rho C_D\,\overline{|\,\mathbf{u}\,|\,\mathbf{u}} \qquad (12)$$

is then approximately linear

$$\bar{\tau}_B \sim \rho K \bar{\mathbf{u}}, \qquad (13)$$

where

$$K \sim C_D \hat{u}_T.$$

This linearity, for these wind stresses, implies that it is generally only necessary to compute distributions of residual currents and sea levels for two wind directions (see Figs. 2, 3, 4, 5) to determine the approximate response for a wind from any other direction. It is also clear that in some regions like the Skagerrak where the tidal currents are very small and where the wind residuals can be very large that frictional effects cannot be linear. In the results presented here bottom friction was used in the quadratic form and all non-linear terms were retained.

Balance of forces

The steady state balance of forces neglecting advection can be written as:

$$\underset{\substack{\text{Coriolis}\\\text{Force}}}{\text{C.F.}} = \underset{\substack{\text{Pressure}\\\text{Gradient}}}{-\text{P.G.}} \quad \underset{\substack{\text{Bottom}\\\text{Friction}}}{-\text{B.F.}} \quad \underset{\substack{\text{Wind}\\\text{Stress}}}{+\text{W.S.}} \tag{14}$$

The ratio E_k, where

$$E_k = \frac{\text{B.F.}}{\text{C.F.}} = \frac{C_D \overline{\mathbf{u}|\mathbf{u}|}}{f h \bar{\mathbf{u}}} \tag{15}$$

determines the relative sizes of the force due to bottom friction with respect to the Coriolis force in the balance of forces. Thus using (13) with tidal currents, $\hat{u}_T$, typically $\hat{u}_T \sim 50\,\text{cm.s}^{-1}$, gives $E_k > 1$ only for water depths less than about ~ 10 m. Alternatively if the tidal currents are negligible in comparison with the wind driven currents then the wind driven current would have to be as large as one knot (in water depths ~ 10 m) for the magnitude of the force due to bottom friction to equal the Coriolis force. In all but the shallowest waters then Coriolis forces will be larger than bottom friction.

In general, contributions from all terms in the balance of forces will be important in determining the wind driven residual currents. It is however instructive to examine the balance between a pair of opposing forces.

● Wasserstau or slope adjustment, PG=W.S.

A sea surface slope will readily develop to balance the wind stress if the sea or bay is essentially blocked at one end and the wind is directed into or out of the region of interest. For example, with a SE wind (or preferably a wind from the SSE) blowing across the North Sea (see Figs. 4 and 5) the sea surface slope, ∇E, will adjust to balance the wind stress with

$$\nabla E = \frac{\tau_w}{\rho g h}. \tag{16}$$

Consider as an example the region in the southern North Sea between the Dogger Bank and the Frisian Isles where the wind residuals are small. The water depth, h, is about 40 m which gives $\nabla E \sim 4 \times 10^{-7}$ as is indeed observed. It should be remembered that small deviations from this result will occur in the real sea due to the vertical circulations induced by the wind stress. Such effects can be examined with a 3-dimensional approach (Heaps, 1974).

● Wind drift C.F.=W.S.

Under more open sea conditions, for example, the southern regions of the Celtic Sea and the northern parts of the North Sea, pressure gradients will not always be able to develop and so the vertically integrated transports will be to the right of the wind direction (see Figs. 2 and 4).

The vertically integrated component of flow at right angles to the wind direction is given by balancing the wind stress against the Coriolis force

$$\mathbf{k} \wedge \bar{\mathbf{u}} \sim \frac{\tau_w}{\rho f h} \tag{17}$$

(where $\mathbf{k}$ is a unit vector in the vertical direction) which in water depths $h \sim 100$ m gives $\bar{\mathbf{u}} \sim 1.5\,\text{cm.s}^{-1}$. In accordance with these considerations a SSW wind (see Figs. 2 and 7) will marginally assist in driving a flow through the Fair Isle Passage whereas a S.E. wind directs more flow into the Celtic Sea and through the Irish Sea *via* the St. Georges Channel (Figs. 4 and 13).

Flow to the right of the wind also occurs over the Dogger Bank with a SE wind (Fig. 4). Although there is an approximate balance between pressure gradient and wind stress in the North Sea under these conditions (see previous section) the wind stress cannot maintain an increased sea surface slope locally over the shallower Dogger Bank so a flow to the right of the wind develops. In this shallow region bottom friction also plays a role and the angle α between the current flow and the wind stress depends on the relative sizes of the Coriolis force and bottom friction, thus

$$\alpha \sim \tan^{-1}\left(\frac{1}{E_k}\right) \sim 68° \tag{18}$$

(using $\hat{u}_T \sim 30\,\text{cm.s}^{-1}$ and $h \sim 17$ m for the shallowest parts of the Bank) which approximates to the maximum modelled deviation of about 60°.

As the flow passes over the Dogger Bank into deeper water continuity requires that the currents decrease. Vorticity will be associated with the water depth variations (see later) and such an effect can be observed between the shallow Dogger Bank and the deeper water regions nearer the East Coast of England where a counter clockwise circulation can be observed.

● Approximate Geostrophic Balance C.F. $\sim$ −P.G.

If the sea surface slope is much larger than the value determined by equation (16) then Coriolis forces are likely to be important. This happens when the land boundaries are unable to contain a balanced sea surface slope. Such an example occurs on a large scale with a SW wind which drives the flow across the North Sea toward the Danish Coast (Fig. 2). The pressure gradient will be unable to balance the wind stress as the flow can leave the Danish Coast by flowing around the Skagerrak and then along the Norwegian Trench. The currents in the Skagerrak and Norwegian Trench can be estimated from the sea surface elevations (Fig. 3) using the geostrophic relation

$$\mathbf{k} \wedge \bar{\mathbf{u}}_g = -g \frac{\nabla E}{f}. \tag{19}$$

Geostrophic flow $\bar{\mathbf{u}}_g$ tends to follow water depth contours since $\nabla\wedge$ of equation (19) implies that

$$\nabla . \bar{\mathbf{u}}_g = 0, \tag{20}$$

and using continuity

$$\nabla . \bar{\mathbf{u}}_g h = 0, \tag{21}$$

gives

$$\bar{\mathbf{u}}_g . \nabla h = 0, \tag{22}$$

which states that $\bar{\mathbf{u}}_g$ and ∇h are perpendicular. The tendency for the flow to be constrained by topography due to Earth's rotation can result in increased flow where water depth contours converge as in deeper water regions near the entrance to the Skagerrak (Fig. 2).

Whilst the Coriolis force and the pressure gradient may be comparable in size, bottom friction and wind stress still largely determine the flow. For example the wind may accelerate a flow along a coastline until a balance

$$\text{B.F.} \sim \text{W.S.}, \tag{23}$$

is achieved if there are no boundaries in the direction of flow for the water to pile up against [although there may be a transverse pressure gradient given approximately by equation (19)]. With bottom friction in the approximate form of (13) gives

$$\bar{u} = \tau_w / (\rho C_D \hat{u}_T), \tag{24}$$

whereas if quadratic friction is more applicable then

$$\bar{u} \sim [\tau_w / \rho C_D]^{1/2}. \tag{25}$$

The appropriateness of (25) under SW wind conditions in the shallow waters of the Skagerrak near the Danish Coast (Fig. 8) where the tidal streams are much smaller than the wind residual currents ($\hat{u}_T \ll \bar{u}$) can be examined by substituting the values of $\tau_w = 1.6$ dynes cm^{-2} and $C_D = 0.0025$ in (25) to give $\bar{u} \sim 26$ cm.s^{-1}. This is close to that actually determined (~ 30 cm.s^{-1}) and suggests a local balance between wind stress and bottom friction in this shallow region. With double the wind stress the flow within 20 n.m. of the Danish Coast in the Skagerrak increases by about $\sqrt{2}$ as expected by the form of (25). This local nonlinearity, however, has little effect on the outflow in the Norwegian Trench at 59°30'N which increases from 1 to 2 Sverdrups (from 0.97 to 1.94 10^6 m^3.s^{-1}) as the wind stress is doubled. This implies that although most of the water flowing out along the Norwegian Trench has passed through the Skagerrak it is not driven locally by the wind stress in this region but determined by conditions in the North Sea as a whole where the model is essentially linear. The response of the flow along the Norwegian Trench at 59°30'N for different wind directions is illustrated in Figure 16 showing that a maximum response occurs for a wind from 228°.

Water depth variations

If the sea region is essentially enclosed and the water depth is approximately constant then the sea surface slope will adjust to a value where it just balances the wind stress and the vertically integrated residual flow falls to zero. This, however, is not possible if water depth variations perpendicular to the wind direction are significant, as they are generally between near shore and offshore regions when the wind direction is along the shore. The wind sets up larger pressure gradients in the shallower waters which cannot be maintained in the deeper offshore regions and so circulations develop with the flow in the direction of the wind near the shore with reduced or return flow in deeper water. Many examples of these shallow water circulations occur in small bays and similar larger scale effects can be observed in Figures 2 and 4, for example, in the northern Irish Sea with a SE wind or the Irish Sea, Celtic Sea and western English Channel with a SW wind. A further effect of water depth variations occurs along the shallow waters off the Danish west coast with a SE wind.

Coriolis forces associated with these circulations will modify the sea surface elevations set up by the wind. It is convenient therefore to analyse these circulations in terms of vorticity thereby eliminating the pressure gradient term (see § wind stress torque below).

Vorticity

● Geostrophic Vorticity

The geostrophic vorticity, $\omega_g = \nabla \wedge \bar{\mathbf{u}}_g$ can be found by applying the operator ∇. to equation (19) (neglecting variations of Coriolis parameter with latitude) to give

$$f\,\mathbf{k}.\nabla \wedge \bar{\mathbf{u}}_g = g \nabla^2 E, \tag{26}$$

or

$$\omega_g = g / f \nabla^2 E. \tag{27}$$

The flow in the Skagerrak entrance with a SW wind is roughly geostrophic and reference to Figure 3 shows that a trough of low pressure occurs near this region. $\nabla^2 E$ is positive at a trough so this region will be associated with positive (cyclonic) relative vorticity, as is indeed observed in Figure 2.

● Wind stress torque

$$\nabla \wedge \frac{\tau_w}{\rho D}.$$

By applying the operator $\nabla \wedge$ to equation (2) and omitting effects due to advecting and stretching relative vorticity and planetary vorticity the steady state vorticity equation reduces to:

$$0 = -\nabla \wedge \frac{\tau_B}{\rho D} + \nabla \wedge \frac{\tau_w}{\rho D}. \tag{28}$$

Then expanding equation (28) and for simplicity using constant linear friction gives

$$0 = -\frac{K}{h}\omega\,\mathbf{k} - \frac{K\bar{\mathbf{u}}}{h^2} \wedge \nabla h + \frac{\tau_w}{\rho h^2} \wedge \nabla h. \tag{29}$$

The first term on the right hand side of (29) represents dissipation of vorticity due to friction, the second term is a term due to the effects of bottom friction in variable water depths and the third term represents the production of vorticity due to the wind stress acting on water columns of variable depth, h. In general the second and third terms will not balance and so an estimate for the vorticity due to wind stress becomes

$$\omega\,\mathbf{k} \sim \frac{\tau_w}{\rho h K} \wedge \nabla h \sim \frac{\tau_w}{\rho C_D \hat{u}_T h} \wedge \nabla h. \tag{30}$$

CONCLUSIONS

A numerical model is used to derive the currents driven by a steady wind stress on the shelf seas around the British Isles. The wind is superimposed on an accurate working model of the M_2 tide. The M_2 tidal flow is in general of larger amplitude than the wind driven residuals and so largely determines the friction in the model. The wind driven residuals are therefore nearly linear with respect to an applied wind stress. This linearity implies that had both M_2 and S_2 tidal constituents been included in the model then the wind driven residuals would be greater at neap tides and smaller at spring tides—a result which is in contrast to the tidally induced residual flows.

Linearity means that it is only necessary to derive the wind driven currents and sea surface elevations for two wind directions to determine the response for a uniform realistic wind stress applied in any direction. Water budgets for the North Sea and the Celtic Sea are determined under steady wind stress conditions. A small correction to these estimates may be necessary due to the effects of the wind stress outside the modelled region. Although uniform steady wind conditions may be rarely realised in nature a SW or WSW wind stress approximates to winter conditions on the NW European shelf. Estimates for the winter transport of water through the Strait of Dover (Prandle, 1978 *b*) are comparable with the transport of $\sim 20\times10^4\,m^3.s^{-1}$ for the SW wind stress illustrated in Figure 2 and so this distribution of wind driven residuals will approximate to the winter pattern of residual flows around the British Isles. The more local circulations will be valid even if the wind stress is not uniform over the whole region provided the wind stress is reasonably uniform over the region of local interest.

REFERENCES

Bowden K. F., 1956. The flow of water through the Straits of Dover related to wind and differences in sea level, *Phil. Trans. R. Soc. London, ser. A*, **248**, 517-551.

Cartwright D. E., 1976. Shelf-Boundary tidal measurements between Ireland and Norway, *Mém. Soc. R. Sc. Liège*, **10**, 133-139.

Flather R. A., 1976. A tidal model of the north-west European Continental Shelf, *Mém. Soc. R. Sc. Liège*, **9**, 141-164.

Flather R. A., Davies A. M., 1975. *The application of numerical models to storm surge prediction*, Institute of Oceanographic Sciences Report, **16**, 49 p.

Heaps N. S., 1974. Development of a three-dimensional numerical model of the Irish Sea, *Rapp. P. V. Réun. Cons. Int. Explor. Mer*, **167**, 147-162.

Heaps N. S., 1978. Linearised Vertically-Integrated Equations for Residual Circulation in Coastal Seas, *Dtsch. Hydrogr. Z.*, **5**, 147-169.

Hunter J. R., 1974. *An investigation into the circulation of the Irish Sea*, Marine Science Laboratories Menai Bridge Report 72-1, 166 p.

Hunter J. R., 1975. A note on the quadratic friction in the presence of tides, *Estuarine Coastal Mar. Sci.*, **3**, 473-475.

Maier-Reimer E., 1977. Residual Circulation in the North Sea due to M_2 tide and Mean Annual Wind Stress, *D. Hydrogr. Z.*, **30**, 69-80.

Oerlemans J., 1978. Some Results of a Numerical Experiment Concerning the Wind Driven Flow through the Straits of Dover, *Hydrogr. Z.*, **5**, 182-189.

Phillips O. M., 1966. *The Dynamics of the upper Ocean*, Cambridge University Press, 261 p.

Pingree R. D., Griffiths D. K., 1978. Tidal fronts on the shelf seas around the British Isles, *J. Geophys. Res.* (Oceans and Atmospheres), Chapman Conference Special Issue, **83**, 4615-4622.

Prandle D., 1978 *a*. Residual flows and elevations in the southern North Sea, *Proc. R. Soc. London, ser. A.*, **359**, 189-228.

Prandle D., 1978 *b*. Monthly-mean residual flows through the Dover Strait, 1949-1972, *J. Mar. Biol. Ass. U.K.*, **58**, 965-973.

Ronday F. C., 1972. *Modèle mathématique pour l'étude des courants résiduels dans la Mer du Nord*, Manuscript Report Series, **27**, Marine Sciences Directorate, Ottawa, 54 p.

Weare T. J., 1975. Mathematical Models, *Consult. Eng.*, **39**, 37-43.

Table 1

Symbols used in the text.

t, time coordinate;
x, y, horizontal spatial coordinates: x east; y north latitude;
E, surface elevation;
h, undisturbed water depth;
$D=h+E$, total water depth;
P_a, atmospheric pressure;
$\mathbf{u}$, horizontal velocity;
$\mathbf{w}_{10}$, wind velocity at a height of 10 m;
$\mathbf{u}_r$, horizontal residual velocity due to wind stress;
$\hat{u}_T$, maximum amplitude of the M_2 tidal streams;
C_D, drag coefficient for bottom stress $=0.0025$;
K_H, horizontal coefficient of diffusion;
C_{10}, drag coefficient for wind stress $\sim 1.3\times10^{-3}$;
Q, vertically integrated volume transport;
g, acceleration due to gravity;
f, Coriolis parameter;
T, M_2 tidal period;
φ, latitude;
Ω, angular velocity of the Earth's rotation;
Θ, wind direction, positive clockwise;
σ, angular frequency;
k, wave number;
τ_B, bottom stress;
τ_w, wind stress;
ρ, density of sea water;
ρ_a, density of air;
$|\ |$ magnitude of;
$-$ overbar denotes time average over one complete tidal cycle;

$$\nabla=\frac{\partial}{\partial x}\mathbf{i}+\frac{\partial}{\partial y}\mathbf{j};$$

$$\nabla^2=\nabla.\nabla \text{ or } \frac{\partial^2}{\partial x^2}+\frac{\partial^2}{\partial y^2};$$

$$\omega\,\mathbf{k}=\nabla\wedge\bar{\mathbf{u}}=\left(\frac{\partial}{\partial x}\mathbf{i}+\frac{\partial}{\partial y}\mathbf{j}\right)\wedge\bar{\mathbf{u}};$$

$\mathbf{i}$, unit vector in the x direction;
$\mathbf{j}$, unit vector in the y direction;
$\mathbf{k}$, unit vector in the vertical direction.